

# EVENTS IN PROTON PUMPING BY BACTERIORHODOPSIN

G. W. RAYFIELD

Physics Department, University of Oregon, Eugene, Oregon 97403

**ABSTRACT** The short-circuit photoresponse of a bacteriorhodopsin-based photoactive membrane is studied. The membrane is formed by first coating a Teflon membrane with lipid and then fusing bacteriorhodopsin vesicles to it. An incandescent light source was used to obtain the rise time of the photocurrent in response to a step-function illumination. A fast response,  $<1$  ms, characterizes the initial rise and decay of the photocurrent. The trailing edge of the rise and trailing edge of the decay each exhibit different time constants both  $>1$  ms. These slower components show a sensitivity to membrane charging, the presence of diethylether in the bathing solution, and the presence of a charged cation complex in the lipid region. The photoresponse is not analyzed by means of the usual equivalent electrical circuit, but rather in terms of image charges in the conducting electrolyte bathing the membrane. Further experiments using a pulsed laser (pulse width  $<1$   $\mu$ s) resolve at least three time constants in the photoresponse: 0.057 ms, 1.06 ms, and 13 ms. Three distinct charge displacements (4.4, 7.5, and 33.1 A) are derived from the data, each corresponding to one of the above time constants.

## INTRODUCTION

Bacteriorhodopsin (BR), which is found in *Halobacterium halobium*, functions as a light-driven proton pump. Studies of the protein may be grouped into four arbitrary areas: the biological role of the protein in the bacteria, the structure of the protein, the photoreaction cycle of the chromophore, and the functional characteristics of the protein as a pump. Recent reviews (1, 2, 3) cover these areas and their interrelations in detail. BR arranged in purple membrane sheets in the cell wall absorbs light and pumps protons, thereby establishing a proton gradient across the cell wall. This process is the basis for photophosphorylation in *Halobacterium halobium*. The protein occurs naturally in an ordered two-dimensional array, the purple membrane sheet. The structure of the protein (MW = 26,000) consists of seven connected  $\alpha$  helices arranged roughly perpendicular to the plane of the membrane with charged amino acid interiors and hydrophobic exteriors (4). The photon absorption site (retinal) is buried in the protein and likely connected through a Schiff base to Lys-216 in the amino acid sequence (5, 6). Upon illumination this chromophore exhibits a temporal change in its absorption spectra known as the photoreaction cycle. Although the cycle is quite complex, it can be characterized by a fast change to a relatively long-lived intermediate state (the M state), where the chromophore absorbs at 412 nm and returns from this state to the ground state (with a time constant of  $\sim 10$  ms). Functional purple membrane fragments in an aqueous environment show a fast release of protons when they are illuminated (formation of the M state) and take up protons when the illumination is turned off (3). The Schiff base is observed to protonate and deprotonate during the course of the photoreaction cycle.

At this time, the information available about the proton

pumping mechanism is insufficient to develop a definitive model at the molecular level, although there is much speculation (3, 7–12). It is now a generally accepted fact that transient electrical signals can be detected from the isolated protein when it is illuminated (2). Whether or not these effects can be interpreted to yield useful information relative to the proton pumping mechanism remains to be seen. Purple membrane fragments have been studied almost exclusively in these experiments, with little or no work reported on the monomeric form of the protein. Early measurements of electrical signals from BR in model systems reflected the behavior of the model system and yielded little information about the movements of charge within the light-activated protein.

Trissl and Montal (13) have reported measurements in which a photoactive membrane was formed by first foaming an aqueous salt solution of purple membrane fragments, then spreading this foam on a water surface, overlaying with hexane, and finally transferring the film to a thin Teflon septum. They report three different time constants for the transient photopotential: 1 ms, 15 ms, and 1 s. Hong and Montal (14), using the same system but different instrumentation, report two peaks in the photoresponse: a positive peak 1.5  $\mu$ s after the light pulse, and a negative peak at 21  $\mu$ s decaying exponentially to the base line with a time constant of 160  $\mu$ s. No components with longer time constants were observed in the photosignal. They report that these time constants depend on the characteristics of the external measuring circuit.

Drachey et al. (15) examined photoresponses (photopotentials) from a membrane formed by first impregnating a collodion film with lipid and then fusing either BR containing vesicles or purple membrane sheets to the film. Four different phases to the photopotential were observed: an

initial negative potential transient was followed by positive transient that exhibited three different phases: one with a time constant from 25–50  $\mu$ s, another with a time constant of 6–12 ms and, finally, a decay of the potential to zero with a 1 s time constant. The authors speculate that these photopotential measurements demonstrate two unidirectional phases of current movement in the protein. In more recent work (16), these same authors along with Khitrina discuss the photopotentials in terms of the protonated Schiff base translocating within the membrane.

Fahr et al. (17) measured photocurrents from a model system consisting of purple membrane sheets attached to a planar lipid bilayer membrane (BLM). They report an initial phase to the phototransient that has a negative amplitude with a time constant of 1.2  $\mu$ s, followed by a positive amplitude component with a 16.9  $\mu$ s time constant, and then one with a 59  $\mu$ s time constant. The longest decay time observed was 940  $\mu$ s. The results are tentatively interpreted in terms of a series of charge displacements within the protein correlated with the photoreaction cycle. These investigators choose to adjust the input impedance of the measuring circuit to that of the membrane and electrolyte; justification and details of this procedure are not given. In particular, they fail to mention whether this procedure is related to the poor signal-to-noise ratio of the instrumentation.

Keszthelyi and Ormos (18) have reported an interesting experiment designed to develop a correlation between electrical signals from the protein and the optical absorption characteristics of the retinal chromophore in the protein. They observe that if purple membrane fragments are suspended in a water bath and two electrodes immersed in the bath are connected to each other through a resistance, a transient voltage appears across the resistance, when the solution is flashed with light (the fragments are oriented by a large DC voltage before the light flash). Time constants for the photoeffect varied from 4.4  $\mu$ s (the minimum rise time of the amplifier) to 8.0 in  $H_2O$ , and to as long as 22 ms in  $D_2O$ . It is not clear from the analysis of the experiment how the transient photoeffects are related to the physical phenomenon of charge movement within the protein. The authors ignore any electrical effect (i.e., shorting) due to the water surrounding the fragments. Correlation between the observed photoeffect and the photoreaction cycle was reported.

One can see from the brief review above that there exists a wide range in the photoresponse time constants reported that reflect the same physical phenomenon. Some speculations can be made in resolving this dilemma and meshing the data into a common framework: (a) long time constants (13, 15) of order seconds probably reflect characteristics of the model system (19); (b) intermediate time constants 1 to 10 ms (13, 18) reflect charge movements within the protein, but are not detected in some experiments (14, 17) due to the low signal level; (c) signals with

fast time constants are not detected in other experiments due to a slow instrumental time constant.

Clearly, precautions must be taken in the design and interpretation of both the experiment and instrumentation so that information derived from the data indeed reflects physical processes occurring within the protein. The simple association of an electrical effect with a displacement current, and the development of an equivalent electrical circuit yields little insight into the light-activated microscopic charge movements within the protein. The analysis presented in the next section is an attempt to make this relationship less abstract and less obscure.

## ANALYSIS

Consider a charge  $q$  placed between two infinite conducting parallel plates of separation  $d$ , a distance  $x$  from one of them. The plates are connected externally through an ideal ammeter (zero internal resistance) so that both plates are always at the same potential. The induced image charges on the plates are  $-(x/d)q$  and  $-([d - x]/d)q$ . If the charge is displaced by an amount  $\delta x$ , then a charge  $\delta q = (\delta x/d)q$  must flow through the external circuit to maintain the boundary conditions. If this takes place in a time  $\delta t$ , then a current  $i = \delta q/\delta t$  flows through the ammeter for a time  $\delta t$ . The rotation of an electric dipole placed between the plates also causes a current to flow in the external circuit. The resulting current is simply the sum of the currents due to the motion of each charge making up the dipole. If the region between the plates is filled with a homogeneous dielectric, the same induced image charge appears on the plates and the current flow in the external circuit is unaffected.

If the external circuit is open, the movement of a charge  $+q$  from  $x$  to  $x + \delta x$  generates a uniform surface charge  $q\delta x/d$  on the plates (to maintain boundary conditions), and a potential between the plates develops. The relation between the short-circuit current  $i = q\delta x/(d\delta t)$  and open-circuit potential  $V$  is given by:  $V = C^{-1} \int i dt$ , where  $C$  is the capacity of the plates. Insertion of a homogeneous dielectric between the plates reduces this potential. The measurement of this potential with a nonideal voltmeter introduces an additional instrumental time constant  $RC$ , where  $R$  is the internal resistance of the voltmeter.

Fig. 1 shows a photon absorption site  $R$  that is located between the plates and ejects a positive charge, creating an electric dipole, when a photon is absorbed.  $A$  is an ideal ammeter shunting the plates. A vectorial property for the site is specified by assuming that the charge released from  $R$  hops to the site  $C$ . This pathway,  $R$  to  $C$ , is taken to be unidirectional so that  $R$  can only receive a replacement charge from site  $A$  along the pathway  $A$ – $R$ . Only positive current transients are registered in the external circuit as  $R$  is cycled and moves charge from  $A$  to  $C$ . If several identical noninteracting photon-receptor sites are contained

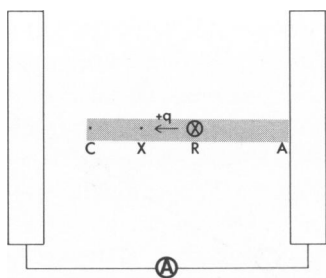


FIGURE 1 Currents registered by an ammeter A connecting two parallel conducting plates due to charge  $+q$  movements in the region between the plates. R is a photon receptor site and trapping sites are located at A, X, and C.

between the plates, the superposition theorem holds and the total current registered by the ammeter is the sum of the partial currents due to each site. The relative position of each site between the plates has no effect on the measured current, while a random vectorial orientation yields zero current.

We assume now that the release of a positive charge from site R after absorption of a photon is characterized by a lifetime  $\tau$ . Then the probability the charge is released in the time interval  $t$  to  $t + \delta t$  is  $\tau^{-1} \exp(-t/\tau) \delta t$ . Let the number of sites excited by a flash of photons at time  $t = 0$  be  $N$ , and assume the time to hop from R to C is small compared with the lifetime  $\tau$ . The partial current registered on the ammeter (Fig. 1) in the time interval  $t$  to  $t + \delta t$  due to the motion of positive charge from R to C is then given by

$$i_1(t) = Nq [\exp(-t/\tau)] \delta x / (d\tau), \quad (1)$$

where  $\delta x$  is the distance from R to C.

If a second event corresponding to a charge movement from A to R is allowed to follow the first, then the total current registered by the ammeter will be the sum of the two partial currents corresponding to the two distinct events. The rate of hopping from R to C and A to R is represented by a set of coupled differential equations that also contain a term representing the driving function (photon flux). It is assumed that A to R occurs only when R is vacant following the R to C transition. Assuming a  $\delta$  function (light flash), the partial current contributed by the first event is that given above, while the second event contributes a partial current

$$i_2(t) = Nq [\exp(-t/\tau') - \exp(-t/\tau)] \delta x' / d(\tau - \tau'), \quad (2)$$

where  $\delta x'$  is the distance from A to R, and  $\tau'$  is the lifetime of this hop. Additional features may be incorporated in the events associated with charge motion between the plates; for example, a trapping site X between R and C may be postulated. Eqs. 1 and 2 also show why sensitive instrumentation is required to record some events, even though the hopping distance is large.

The movement of charge from A to C through the photon absorption site leads to a net buildup of charge at site C. If the dielectric is slightly conductive, then a tiny leakage current between C and one or both of the conducting plates can develop. If this leakage current is small enough, then the lifetime of C is very long compared to other time constants in the problem; and, for short times, the short-circuited current reflects only the movement of charge from A to C.

Inhomogeneous regions of dielectric, isolated, conducting regions and isolated static charges distort the electric field lines between the plates. This creates a more difficult electrostatic problem that must be considered in a more rigorous treatment and would lead to a correction term for the relative hop distance.

## EXPERIMENT

The photoactive protein, BR, in the form of purple membrane sheets was derived from a *Halobacterium halobium* culture following standard procedures (20, 21). Strain R1 of *Halobacterium halobium* was kindly supplied by Dr. W. Stoekenius, University of California at San Francisco, and the culture was grown again following standard procedures. Fresh protein was prepared every few months and kept at 4°C in distilled water (with 0.1% Na<sub>2</sub>S<sub>2</sub>O<sub>3</sub>) until needed. Other materials and chemicals were obtained from standard sources. Azolectin (soybean), carbonylcyanide *m*-chlorophenylhydrazone, and valinomycin were obtained from the Sigma Chemical Co., St. Louis, MO. The azolectin was further purified following the method of Szabo et al. (22). Bovine phosphatidylserine was purchased from Avanti Biochemicals, Inc., Birmingham, AL, and diethylether was obtained from the J.T. Baker Chemical Co., Phillipsburg, NJ.

The photoactive membrane was formed on a solid 6  $\mu\text{m}$  thick (area = 0.68  $\text{cm}^2$ ) Teflon septum that separated two chambers containing aqueous salt solutions. The following procedure was used for forming the membrane: 5–10  $\mu\text{l}$  of a charged phospholipid mixture is used to coat the Teflon septum, while it is in contact with the bathing solutions. This lipid mixture consists of phosphatidylserine and azolectin (ratio 3:7 wt/wt) added to decane (10 mg/ml). A mixture of the same lipids in the same ratio is mixed with distilled water (10 mg/ml), buffered to pH 7 with 10 mM PIPES; purple membrane fragments are then added (1 mg/ml) and the mixture is sonicated on ice for 10 min to produce BR vesicles. 200  $\mu\text{l}$  of this vesicle solution is added to the chamber (15  $\text{cm}^3$  vol) containing 100 mM NaCl, 10 mM CaCl<sub>2</sub>, and 5 mM PIPES (pH 7). The vesicles are allowed to fuse with the lipid-coated Teflon septum for ~2 h. The bathing solution containing vesicles is then drained and replaced. The resulting photoactive membrane is rugged and therefore stable for a period of several days. Somehow, for reasons not clear at this time, the procedure results in a net orientation of the protein on the substrate. Perhaps this is related to the observation by van Dijk et al. (23) that small (sonicated) BR vesicles show orientation approaching 90%. In earlier work (24), photoactive model membranes formed using this technique were compared with model membranes based on a BLM. This paper also contains additional information on the procedure.

Silver-AgCl electrodes immersed in the electrolyte provide electrical contact to the external circuit (ammeter). The ammeter in the external circuit ideally has zero impedance. This can be closely approximated by using a high-quality operational amplifier in a current to voltage configuration. The feedback resistor,  $R_f$ , has to be shunted by a suitable capacitance  $C_f$  to compensate for the pole introduced by the membrane capacitance. The approximate value of  $C_f$  for critical damping is given by (25):  $RC_f = 2(RC/2\pi\nu_0)^{1/2}$ , where  $C$  is the input (membrane) capacitance and  $\nu_0$  is the frequency at which the operational amplifier's (op

amp's) open-loop gain is unity. The circuit rise time is then given by  $RC/2$ . These expressions are derived by assuming  $C_f$  is small compared with  $C$  and has a large DC open-loop gain. The input capacitance of the Teflon membrane described above is  $\sim 250$  pF. The current-to-voltage converter was constructed using an Analog Devices, Inc. (Norwood, MA, model 42L) operational amplifier. The op amp has  $\nu_o = 1$  M Hz so that a  $10^7$  ohm feedback resistor requires a 4 pF capacitor for critical damping and gives a rise time of 20  $\mu$ s. This predicted rise time was consistent with measured values using suitable test circuits (24). The measured rms current noise was 100 pA. A low-pass filter ( $f_o = 2,000$  Hz) was often used in conjunction with the ammeter to improve the signal to noise ratio.

The output from the ammeter is fed into an analog-to-digital converter (ADC) and stored as data files on floppy disks using a PDP-11 computer (Digital Equipment Corp., Maynard, MA). Software programs were used for signal averaging, digital averaging, or to analyze the data files. Software also controlled the synchronization of the light source. The ADC was limited to an acquisition time of 30  $\mu$ s.

Two light sources were used for illuminating the membrane: an incandescent lamp with an electric shutter (rise time 0.7 ms) for a step function, or a pulse laser (Phase-R Company, model DL-2100A, 10 mJ to 3 J per pulse) for an impulse function. The incandescent source consists of a 150 W projector lamp with a regulated DC power supply and glass filters to restrict the pass band. The light intensity at the membrane was measured by installing a calibrated photodiode behind the membrane; careful adjustment of the optics gave a steady membrane illumination of 97 mW/cm<sup>2</sup>. The intensity could be doubled by including a mirror behind the membrane. Lower intensities were obtained by the use of neutral density filters.

## RESULTS

A series of measurements were performed on photoactive membranes prepared as described above. The incandescent light source was used for the time domain above 1 ms and the pulsed laser source for the region below 1 ms. Only short-circuit current measurements were made; the ammeter shorted the two salt solutions bathing the membrane. All measurements were made with the bathing solutions buffered to pH 7 and at room temperature 23°C. Except as otherwise noted, the bathing solutions contained 100 mM NaCl, 10 mM CaCl<sub>2</sub>, and 5 mM PIPES.

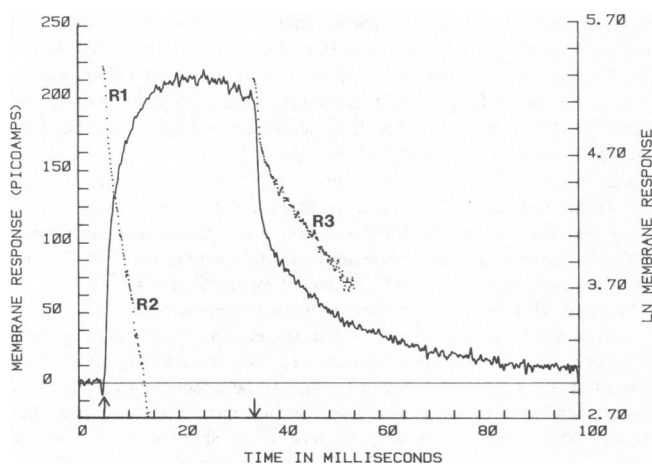


FIGURE 2 The short-circuit photocurrent of a photoactive membrane formed from BR protein and lipids on a Teflon substrate is shown. The points are the log of the photocurrent and three rate constants  $R1$ ,  $R2$  and  $R3$  are identified in the log plot.

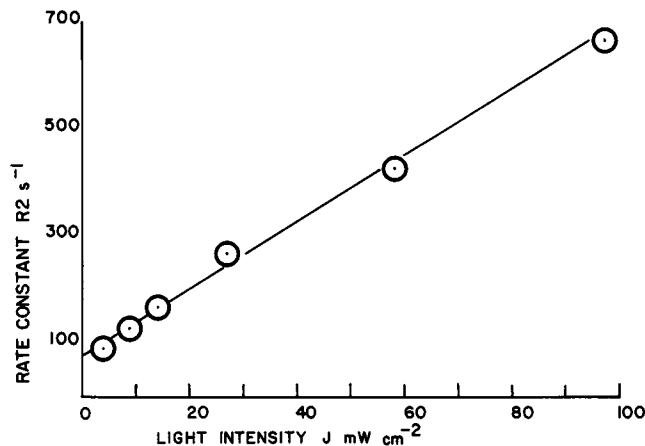


FIGURE 3 The variation of the rate constant  $R2$  (the trailing edge of the photocurrent rise, see text) with light intensity is shown.

The short-circuit current photoresponse of a membrane prepared as described above is shown in Fig. 2 for the time domain from 1 to 100 ms; a current measurement was made every 100  $\mu$ s by the ADC. This time domain encompasses the overall time scale of the photoreaction cycle of BR, which is  $\sim 10$  ms. The shutter was open for 30 ms and light intensity was 27 mW/cm<sup>2</sup>. The light was left on long enough that a base line for the on response could be obtained; using this base line and the zero-current base line for the off response, the log of the photoresponse was calculated and is shown by the points in Fig. 2.

Fig. 2 illustrates a characteristic asymmetrical feature of the photoresponse curve; the rise time is different than the decay time. Another feature is also apparent in the data; neither the rise nor the decay portions of the photoresponse is a simple exponential. Three regions with different time constants can be identified in the short-circuit photoresponse. A fast response of  $<1$  ms characterizes the initial rise and decay of the photoresponse curve. This rate constant is designated  $R1$ . The trailing edge of the rise exhibits a rate constant,  $R2$ , that is dependent on light intensity (Fig. 3). The trailing edge of the decay is characterized by a rate constant  $R3 \approx 70$  s<sup>-1</sup> that is light independent except for long, intense light pulses. At high light intensity, the photoresponse begins to decay before the illumination is turned off. This is possibly due to membrane charging<sup>1</sup> and/or depletion of the chromophore ground state (i.e., light saturation). This effect has not yet been studied in detail.

Fig. 4 shows the photoresponse to a short (5 ms), high intensity (97 mW/cm<sup>2</sup>) light pulse. Again, the points are the logarithm of the photoresponse curve. The peak current (base line for the on-response) was estimated using a slightly longer light pulse. The short-circuit photocurrent decays slowly to the base line with no evidence of a

<sup>1</sup>Charging of the membrane may lead to a potential bias across the pump current because of its voltage dependence (19).

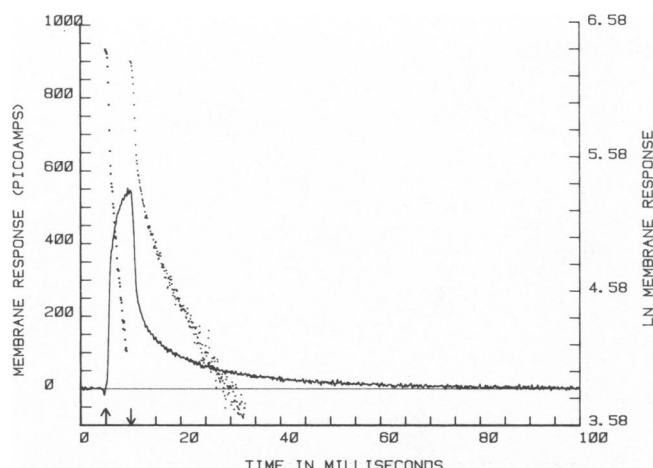


FIGURE 4 The short-circuit photoresponse to a 5 ms light pulse is shown; the points are the log of the photoresponse. The experimental conditions are the same as those of Fig. 2.

negative current component. Significantly increasing the length of the light pulse and its intensity caused a noticeable increase in the rate constant  $R3$  as  $R1$  remained  $<1$  ms. This result suggests that  $R3$  might be sensitive to an electrical potential bias across the protein.<sup>2</sup>

Charging the photoactive membrane by full illumination immediately before a photoresponse is taken leads to the short-circuit photoresponse shown in Fig. 5 (solid line). The membrane was charged by first illuminating it until the photoresponse current was zero; the light was then turned off and the photoresponse was measured after waiting  $\sim 2$  s. The data shown in Fig. 5 (solid curve) were taken using a 5 ms long light pulse of maximum intensity ( $97 \text{ mW/cm}^2$ ). The regions of the photoresponse curve associated with the rate constants  $R2$  and  $R3$  have been virtually eliminated by charging the membrane. After a longer wait, the membrane completely discharges and the original photoresponse (dotted curve, Fig. 5) is recovered. These results suggest that the photoresponse curves in Figs. 2 and 4 are really composed of two different components, and that one component, the slow one, is sensitive to potential bias across the membrane, whereas the fast component associated with  $R1$  is less sensitive to bias potential.

Diethylether is one of several chemical agents that has been shown to have an effect on the photoreaction cycle (26, 1). The aqueous solution bathing the membrane, in the experiment reported here, was completely saturated with ether by adding diethylether to the solution until an undissolved layer of ether  $\sim 1/4$  in. deep covered the surface. The solution was then stirred using a magnetic stirrer until immediately before the measurement. The photoresponses of an ether-treated membrane (peak light intensity  $97 \text{ mW/cm}^2$ ) are shown in Fig. 6 (solid curve) for a 5 ms and

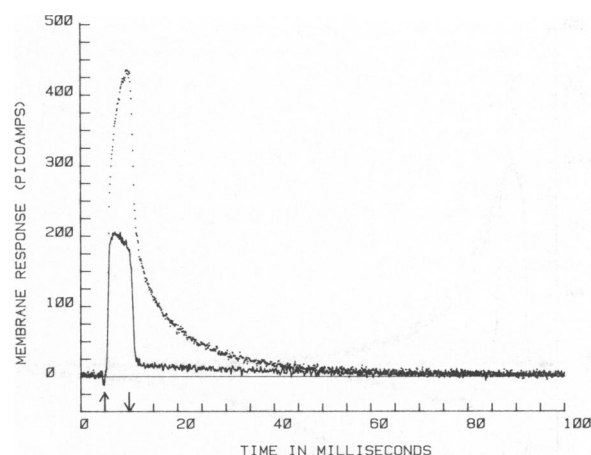


FIGURE 5 The short-circuit photoresponse of a charged membrane is shown. The solid curve is the photoresponse of a previously illuminated membrane that has only been in the dark for a few seconds. The dotted curve is the photoresponse of a membrane that has been in the dark for several minutes.

a 30 ms light pulse. Qualitatively, the difference between the fast component and the slow component is much more visible in the ether-treated membrane than in an untreated membrane (dotted curve, Fig. 6). The characteristic rate constant  $R1$  is relatively unaffected, while  $R2$  decreases to  $400 \text{ s}^{-1}$  and  $R3$  decreases to  $27 \text{ s}^{-1}$ . The trailing edge of the long (30 ms) light-pulse photoresponse is visibly distorted from a true exponential in Fig. 6. In fact, a considerable positive current continues to flow even 65 ms after the illumination is turned off. Allowing the ether to completely evaporate over a period of 2 h restores the original photoresponse of the membrane (dotted curve, Fig. 6), but with a

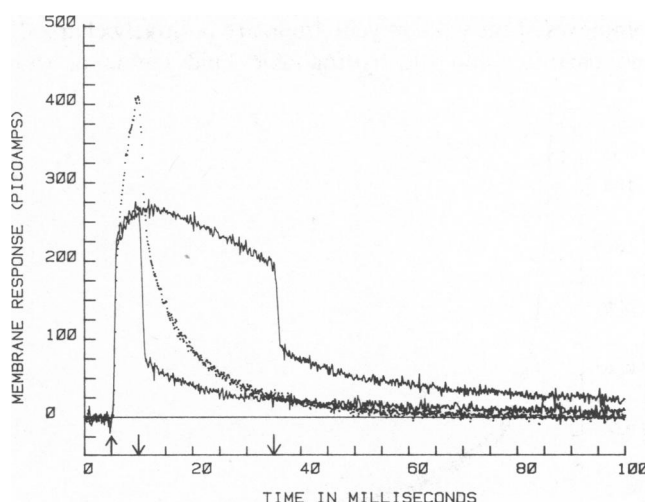


FIGURE 6 The solid lines show the photoresponse to a 5 ms and 30 ms light pulse of the photoactive membrane in a diethylether saturated bathing solution. The photoresponse of the membrane before adding ether is shown by the dotted curve. After evaporation of the ether, the photoresponse was the same as the dotted curve, but reduced in amplitude by about 10%.

<sup>2</sup>This could be a pH effect rather than a potential (electrostatic) effect, even though a buffered bathing solution was used.

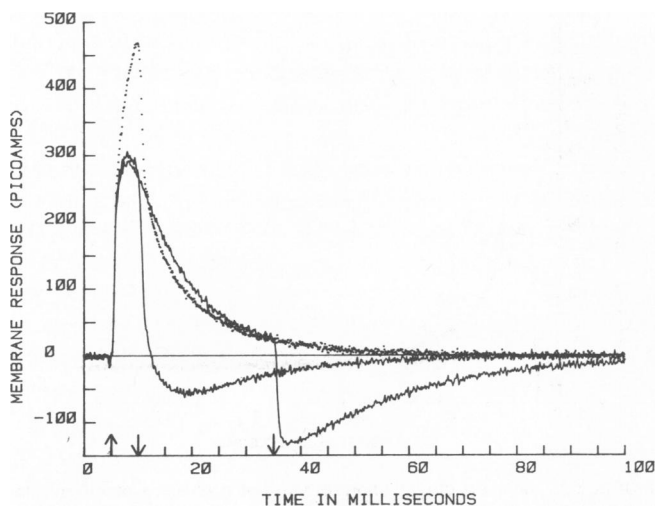


FIGURE 7 The photoresponse (solid line) of the photoactive membrane in the presence of  $0.18 \mu\text{M}$  valinomycin is shown for two different light pulses; one 5 ms long and the other 30 ms long, each having an intensity of  $97 \text{ mW}/\text{cm}^2$ . The dotted curve shows the photoresponse of the membrane without valinomycin. The bathing solution required 6 mM KCl in addition to the other salts (see text) for valinomycin to have an effect.

slightly diminished amplitude;  $R_1$ ,  $R_2$ , and  $R_3$  return to their original values.

Adding the antibiotic valinomycin to a bathing solution containing KCl in addition to NaCl and buffer gave the dramatic change in the photoresponse shown in Fig. 7. The dotted curve shows the photoresponse of the membrane before adding valinomycin (5 ms light pulse maximum intensity) and the solid curves are the photoresponses to 5 and 30 ms light pulses in the presence of valinomycin (maximum light intensity). The valinomycin concentration was  $0.18 \mu\text{M}$ , and 6.7 mM KCl was required for an observable effect on the photoresponse. Alkali-metal cation complexes of the valinomycin group are positively charged and partition into the hydrophobic lipid region of the

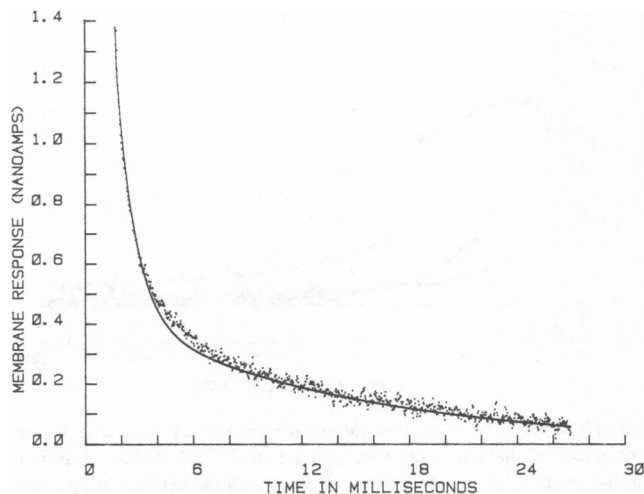


FIGURE 8 The short-circuit photocurrent in response to a laser flash is shown on a relatively long time scale 30 ms.

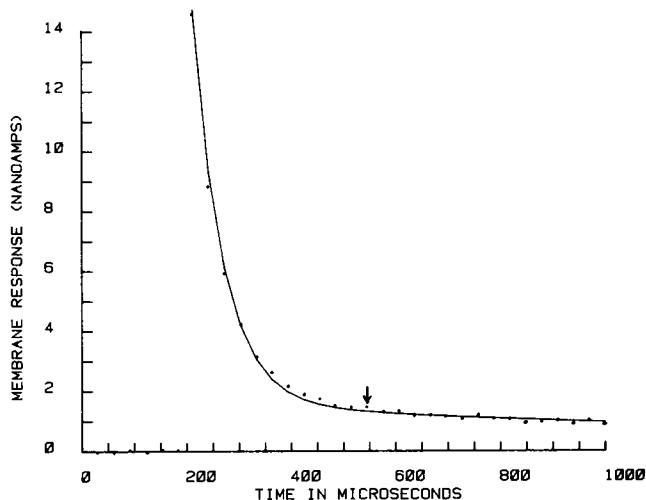


FIGURE 9 The same data as Fig. 8 is shown, but on a short time scale, 1 ms. The arrow marks the beginning of the data shown in Fig. 8.

membrane (27). The fast component of the photoresponse is unaffected by the presence of the cation complex in the lipid, while the slower component is shunted out. The development of a large negative current transient is also evident in Fig. 7.

The short-circuit photoresponse to an impulse-driving function is obtained by photoexciting the membrane with the pulsed laser; a typical response is illustrated in Fig. 8. Data points are taken every  $30 \mu\text{s}$ , the maximum speed of the ADC. The low-pass filter is removed from the measuring circuit and a  $10^7 \Omega$  feedback resistor is used so that the rise time of the ammeter is  $<20 \mu\text{s}$ . The data was smoothed using a digital average that improved the signal-to-noise ratio by about a factor of 2. Fig. 9 shows the same photoresponse (raw data, no smoothing) in the time domain below 1 ms. The solid line in both figures is an empirical fit to the equation

$$I(t) = 13.08 \exp(-t/0.057) + 1.17 \exp(-t/1.06) + 0.43 \exp(-t/13), \quad (3)$$

where  $I$  is in nanoamperes and  $t$  in milliseconds. Due to the slow transient response of the ammeter ( $20 \mu\text{s}$ ), the negative transient reported by other investigators (14, 16, 17) was not studied. The negative transient may be due to a small, fast movement of negative charge in the immediate vicinity of the chromophore.

## DISCUSSION

The experiment results described above can be analyzed in terms of the model presented in the analysis section. This model is a lowest order approximation to the membrane formed as described in the experiment section. The electrolyte solutions bathing the membrane represent the parallel conducting plates in the model. The Teflon substrate and the lipids coating the substrate are taken as part of the homogeneous dielectric along with certain insulating

regions of the protein. The effect of regions of electrolyte that may be trapped within the membrane structure is neglected. The photon absorption (or receptor) site R is taken to be retinal in the protein. C is taken to be one terminal end of a conducting pathway in the protein, and A the other; protons are taken up at A (assumed to be in intimate contact with a proton reservoir, the bath) and released at C as the chromophore (R) is photocycled. The conducting pathways between A and R and R and C are not identified with any particular regions of the protein at this point. We also allow for the possibility of proton traps, such as X in the pathways, with each trap having a characteristic lifetime.

The data shown in Fig. 2–4 show two characteristic features of the short-circuit photocurrent: (a) the rise and fall of the photoresponse are not simple exponentials; both a fast and slow time constant are present; (b) the curves are not symmetrical, the rise time is light intensity-dependent while the fall time is not. These results can be fit into the framework of the model in Fig. 1. The observed deprotonation (fast) of the Schiff base in BR upon photon absorption (3) suggests that R ejects a proton upon photon absorption. The photoresponse then suggests a fast movement of charge (short lifetime) from R to C precedes the slow movement of charge from A to R (long lifetime). The reverse order of events cannot be true because in that case, only one time constant (the slower one) would appear.

The data shown in Figs. 2 and 4 show no evidence of an observable negative current component corresponding, say, to the movement of charge from C to A. A negative current component can, however, be induced by first illuminating the membrane (at maximum intensity) for a long period of time and then following the photocurrent when the light is turned off. This presumably fully charges the membrane by accumulating large amounts of charge at C. Turning the light off then shuts off the movement of charge from R to C in times on the order of 10 ms. The slow leakage of charge from C back to A (or possibly R) shows up as a small leakage current (negative) with a very large decay time of  $\sim 1/5$  s. The sensitivity and the time constant of the experimental apparatus had to be increased for these measurements. A similar measurement of the membrane time constant has been made on the BLM system and yields similar values (28,19). These results indicate that the back leakage of charge from C to A can be neglected for short light pulses in the time domain below 100 ms.<sup>3</sup>

Under the conditions used to obtain the data in Fig. 5, the chromophore is cycled many times (thereby accumulating charge at C) before a photoresponse curve is taken. Within the framework of the model, these data indicate that the hop from A to R is more sensitive to accumulated protons at C than the hop from R to C. Because the origin

of the driving potential for the hop from A to R is unknown, the mechanism of the effect is open to speculation. It may involve electrostatic or pH effects on the chromophore or groups forming the proton channel from A to R.

The data in Fig. 6 show that saturating the bathing solutions with diethylether increases the time constants for hopping from R to C and A to R. Its effect on the photoreaction cycle has been discussed in the literature (1) and is known to slow down the reprotonation of the Schiff base after photoexcitation of the protein (26). This can be interpreted to mean that the hop from A to R is associated with reprotonation of the Schiff base. The mechanism by which ether acts on BR is not known; it may affect the hopping lifetime from A to R directly, and the photoreaction cycle indirectly, or vice versa. The observation that the photoactive membrane can be subject to relatively harsh chemical treatment and still function suggests that a wide variety of chemical modifications can be performed on the protein in situ without destroying the membrane. In some experiments, the bathing solution was completely removed, thereby exposing the surface of the membrane to air; after replacing the original bathing solutions, good photoresponse curves were obtained (although somewhat diminished in amplitude).

When valinomycin and potassium chloride are added to the bathing solution they form a charged cation complex that resides in the lipid region surrounding the protein (27). This alkali-metal cation complex is free to move within the dielectric (lipid) of Fig. 1 and will, therefore, respond to electric fields within the membrane and register as a partial current in the ammeter of the external circuit. The cation distributes itself so as to generate a uniform potential within the membrane; the partial current contributed by the cation motion tends to cancel those partial currents due to other charge motions in the membrane. The continued presence of a large positive transient in the photoresponse (Fig. 7) indicates that lifetime associated with the hop from R to C is faster than the response time of the alkali-metal cation complex. The absence of the slow transient indicates the response time of the cation complex is faster than the lifetime of the hop from A to R. If the hop from A to R is driven by an electric potential gradient in the protein, then the presence of the cation would inhibit the event A to R. An effect due to alkali-metal ion complexes on the photoreaction cycle has been observed (29).

The photoresponse (Figs. 8 and 9) to a laser flash is empirically fit by a sum of three exponentials (Eq. 3). According to the analysis, it follows that another hop might occur in the cycle R to C, A to R. We will call the site associated with this hop X and assume it is located between R and C, although it could equally well be located between A and R. We assume that the sequence of charge hops that occurs when the protein is photocycled is linear: first R to X, then X to R, and finally A to R.

<sup>3</sup>The area under the curve in Fig. 4 is approximately 8 pC so that the peak negative current corresponding to back leakage from C to A is about 5 pA, which is negligible on the scale of Fig. 2.

Because the time constants associated with each exponential in Eq. 3 are quite different (by a factor of 10 or more), the equations in the Analysis section are simplified. The sum of Eqs. 1 and 2 is the short-circuit current that would be observed if only two hops were involved in the photocycling of the protein. Let subscript 1 be associated with the first hop, and subscript 2 with the subsequent hop. If  $\tau_1 \ll \tau_2$ , then this may be written

$$i(t) = i_1(t) + i_2(t) \\ = (Nq/d) [\delta x_1 \tau_1^{-1} \exp(-t/\tau_1) + \delta x_2 \tau_2^{-1} \exp(-t/\tau_2)]. \quad (4)$$

If  $\tau_1 \gg \tau_2$ , then the expression for  $i(t)$  in Eq. 4 would involve only one exponential and the hop distance would be  $\delta x_1 + \delta x_2$ , assuming the partial current  $i_1(t)$  is always associated with the first hop. Extension of the analysis to include an additional site X between R and C is straightforward, and the total short-circuit current becomes

$$i(t) = Nq/d \sum_{j=1}^3 \delta x_j \tau_j^{-1} \exp(-t/\tau_j), \quad (5)$$

where  $N$  is the number of photoreceptors excited by the light pulse,  $q$  is the elementary unit of charge,  $\delta x_j$  is the hopping distance of a particular hop,  $d$  is the dielectric thickness,  $\tau_j$  is the lifetime associated with the particular hop, and  $j = 1, 2, 3$  correspond to the hops from R to X, X to C, and A to R, respectively. Comparison of the exponential factors in Eqs. 3 and 5 gives the lifetimes of the charge hopping events involved in the photocycling of the protein.

A comparison of the amplitudes of the exponentials in Eqs. 3 and 5 allows a value for the relative distance ( $\delta x_j$ ) of each hop to be determined. If the total thickness of the protein is taken to be 45 Å, and assuming that this represents the sum of the three hops,<sup>4</sup> then  $\delta x_1 = 4.4$  Å,  $\delta x_2 = 7.5$  Å, and  $\delta x_3 = 33.1$  Å corresponding to the three time constants  $\tau_1 = 0.057$  ms,  $\tau_2 = 1.06$  ms, and  $\tau_3 = 13$  ms, respectively. Recent work (5, 6) shows that the retinal chromophore is attached to Lys-216 in the protein. This indicates (4) that it is buried in the protein, but also suggests that  $(\delta x_1 + \delta x_2) > \delta x_3$  in contrast to the above.

Some investigators assume a priori that a correlation exists between the various absorption states of the chromophore (photoreaction cycle) and the hopping events in charge movement from A to C during photocycling of the protein (1, 17, 18); others question this assumption. Several of the experiments discussed in the Introduction present evidence for this correlation. The reason for this correlation between the photoreaction cycle and the hopping events of proton translocation through the protein is not particularly transparent. An overall correlation exists within the framework of the model presented in the Analysis because it is assumed that A to R cannot occur until the site R is vacated; one could speculate that the

transition from the M state to the ground state in the photoreaction cycle correlates with the arrival of a proton from A. In the analysis above, the lifetimes of the sites at R, X, and A are assumed to be fixed in time so that the probability of a hop in the time interval between  $t$  and  $t + \delta t$  shows simple exponential behavior. The absorption states of the photoreaction cycle are due to electronic transitions in the chromophore that are sensitive to the surrounding structural environment. It is possible that the structural environment around the chromophore correlates in some way with the movement of charge between sites.

There is another way (rather than postulating the site X) of interpreting the additional exponential term in Eq. 3: The lifetime associated with the hop from R to C might change due to temporal structural changes at R; these changes are also responsible for the variation in the absorption spectra of the chromophore (photoreaction cycle). This leads naturally to a correlation between the photoreaction cycle and the hopping events.

An estimate of  $N$ , the number of proteins on the Teflon substrate, can be made by setting  $d = 6 \times 10^{-6}$  m (the thickness of the Teflon support),  $q = e$  (the unit of elemental charge), and Eq. 4 with the result that  $N = 4 \times 10^{10}$ . This is approximately the total number of proteins in the membrane, assuming saturation by the laser light pulse. The light saturation was checked using neutral density filters. It follows that  $\sim 0.3\%$  of the membrane area is covered by protein.

This work was supported by National Institutes of Health grant GM 26669.

Received for publication 28 December 1981 and in revised form 1 July 1982.

## REFERENCES

1. Stoerkenius, W., R. H. Lozier, and R. A. Bogomolni, 1979. Bacteriorhodopsin and the purple membrane of halobacteria. *Biochim. Biophys. Acta*. 505:215-278.
2. Eisenbach, M., and S. R. Caplan, 1979. The light-driven proton pump of *Halobacterium halobium*: mechanism and function. *Curr. Top. Memb. Transp.* 12:166-248.
3. Bogomolni, R. A. 1980. Conversion of light energy into a proton electrochemical potential by bacteriorhodopsin. In *Bioelectrochemistry*. H. Kayzer and F. Gutmann, editors. Plenum Publishing Corp., New York. 83-95.
4. Engelman, D. M., R. Henderson, A. D. McLachlan, and B. A. Wallace. 1980. Path of the polypeptide in bacteriorhodopsin. *Proc. Natl. Acad. Sci.* 77:2023-2027.
5. Lemke, H. -D., and D. Osterhelt. 1981. Lysine 216 is a binding site of the retinyl moiety in bacteriorhodopsin. *FEBS (Fed. Eur. Biochem. Soc.) Lett.* 128:255-260.
6. Katre, N. V., P. K. Wolber, W. Stoerkenius, and R. M. Stroud. 1981. Attachment site(s) of retinal in bacteriorhodopsin. *Proc. Natl. Acad. Sci.* 78:4068-4072.
7. Lewis, A., M. A. Marcus, B. Ehrenberg, and H. Crespi. 1978. Experimental evidence for secondary protein-chromophore interactions at the Schiff base linkage in bacteriorhodopsin: molecular mechanism for proton pumping. *Proc. Natl. Acad. Sci.* 75:4642-4646.
8. Crespi, H. L., and J. R. Ferraro. 1979. Active site structure of

<sup>4</sup>Hops with very short time constants must have extremely large amplitudes (Eq. 3) to contribute a significant hop distance (Eq. 5).



- bacteriorhodopsin and mechanism of action. *Biochem. Biophys. Res. Commun.* 91:575-582.
9. Karvaly, B. 1980. Bacteriorhodopsin: photochemistry and energy conversion. *Biochem. Biophys. Res. Commun.* 93:1044-1050.
  10. Merz, H., and G. Zundel. 1981. Proton conduction in bacteriorhodopsin via a hydrogen-bonded chain with large proton polarizability. *Biochem. Biophys. Res. Commun.* 101:540-546.
  11. Nagle, J. F., and M. Mille. 1980. Molecular models of proton pumps. *J. Chem. Phys.* 74:1367-1372.
  12. Nagle, J. F., H. J. Morowitz, and M. Mille, 1979. Theory of hydrogen bonded-chains in bioenergetics. *J. Chem. Phys.* 72:3959-3971.
  13. Trissl, H. -W. and M. Montal. 1977. Electrical demonstration of rapid light-induced conformational changes in bacteriorhodopsin. *Nature (Lond.)*. 266:655-657.
  14. Hong, F. T. and M. Montal. 1979. Bacteriorhodopsin in model membranes. A new component of the displacement photocurrent in the microsecond time scale. *Biophys. J.* 25:465-472.
  15. Drachev, L. A., A. D. Kaulen, and V. P. Skulachev. 1978. Time resolution of the intermediate steps in the bacteriorhodopsin-linked electrogenesis. *FEBS (Fed. Eur. Biochem. Soc.) Lett.* 87:161-167.
  16. Drachev, L. A., A. D. Kaulen, L. V. Khitrina, and V. P. Skulachev. 1981. Fast stages of photoelectric processes in biological membranes. *Eur. J. Biochem.* 117:461-470.
  17. Fahr, A., P. Lauger, and E. Bamberg. 1981. Photocurrent kinetics of purple-membrane sheets bound to planar bilayer membranes. *J. Memb. Biol.* 60:51-62.
  18. Keszthelyi, L., and P. Ormos. 1980. Electric signals associated with the photocycle of bacteriorhodopsin. *FEBS (Fed. Eur. Biochem. Soc.) Lett.* 109:189-193.
  19. Herrmann, T. R., and G. W. Rayfield. 1978. The electrical response to light of bacteriorhodopsin in planar membranes. *Biophys. J.* 21:111-125.
  20. Oesterhelt, D., and W. Stoeckenius. 1974. Isolation of the cell membrane of *Halobacterium halobium* and its fractionation into red and purple membrane. *Methods Enzymol.* 21:667-678.
  21. Becher, B. M., and J. Y. Cassim. 1975. Improved isolation procedures for the purple membrane of *Halobacterium halobium*. *Prep. Biochem.* 5:161-178.
  22. Szabo, G., G. Eisenman, and S. Ciani. 1969. Methods of purification of phosphatidyl choline. *J. Membr. Biol.* 1:346-382.
  23. van Dijk, P. W. M., K. Nicolay, J. Leunissen-Bijvelt, K. Van Dam, and R. Kaptein. 1980. <sup>31</sup>P-nuclear magnetic resonance and freeze-fracture electron microscopic studies on reconstituted bacteriorhodopsin vesicles. *Eur. J. Biochem.* 117:639-645.
  24. Rayfield, G. W. 1982. Kinetics of the light-driven proton movement in model membranes containing bacteriorhodopsin. *Biophys. J.* 38:79-84.
  25. Wing, W. H., and T. M. Sanders, Jr. 1967. FET operational amplifiers as fast electrometers. *Rev. Sci. Instrum.* 38:1341-1342.
  26. Oesterhelt, D., and B. Hess, 1973. Reversible photolysis of the purple complex in the purple membrane of *Halobacterium halobium*. *Eur. J. Biochem.* 37:316-326.
  27. Simon, W., and W. E. Morf. 1973. Alkali cation specificity of carrier antibiotics and their behavior in bulk membranes *In* Membranes. G. Eisenman, editor. Marcel Dekker, Inc., New York. 2:329-375.
  28. Bamberg, E., H. -J. Apell, N. A. Dencher, W. Sperling, H. Stieve, and P. Lauger. 1979. Photocurrents generated by bacteriorhodopsin on planar bilayer membranes. *Biophys. Struct. Mech.* 5:277-292.
  29. Avi-Dor, Y., R. Rott, and R. Schnaiderman. 1979. The effect of antibiotics on the photocycle of purple membrane suspensions. *Biochem. Biophys. Acta.* 545:15-23.